Disentangling vibrationally-dependent molecular dynamics in mutual neutralisation reactions

Mathias Poline[1†], Arnaud Dochain[1,2†], Stefan Rosén[1], MingChao Ji[1], Henrik Cederquist[1], Henning Zettergren[1], Henning T. Schmidt[1], Mats Larsson[1], Shaun G. Ard[3], Nicholas S. Shuman[3], Albert A. Viggiano[3], Richard D. Thomas[1*†]

[1]Department of Physics, Stockholm University, Stockholm, SE-10691, Sweden.
[2]Institute of Condensed Matter and Nanosciences, Université Catholique de Louvain, Louvain-la-Neuve, B-1348, Belgium.
[3]Space Vehicles Directorate, Air Force Research Laboratory, Kirtland AFB, Albuquerque, 87117, New Mexico, USA.

*Corresponding author(s). E-mail(s): rdt@fysik.su.se;
Contributing authors: mathias.poline@fysik.su.se;
arnaud.douchain@fysik.su.se,arnaud.douchain@uclouvain.be;
†These authors contributed equally to this work.

Supplementary Materials

Supplementary text concerning: Data evaluation, two-body analysis, three-body analysis, three-body reaction dynamics, the free-rotor model in two-step reactions vibrational cooling.
Figs. S1 to S2
No new references

1 Data evaluation

In order to evaluate the data, appropriate methods must be used to determine the momentum vectors and energies of the products, and Monte Carlo simulations of the particles trajectories must be implemented. The reaction can in principle lead to both two- and three-body products, and these are treated independently.

1.1 Two-body analysis

In a two-body scenario, i.e reaction (1a) in the main text, both products receives a fixed amount of energy, and the calculation of their final kinetic energy and momentum vectors is straightforward (see, e.g. (see, e.g. [6,8]. The resultant experimental 2-body E_{K_f} spectrum for the MN of $^{16,16}O_2^+$ with O^- is shown in fig. S1, plotted as filled black circles with statistical error bars. As the MCP detection efficiency is not 100%, three-body events in which one particle is not detected, but which still satisfies center-of-mass filtering, contribute to the 2-body E_{K_f} data. This contribution can be evaluated by randomly selecting two products out of the three from the three-body data presented in the main article in fig. 1, and these data are indicated by the grey filled circles in fig. S1 here. Comparison of these two datasets allows the true, two-body E_{K_f} spectra to be determined.

While analysis of the 2-body E_{K_f} data plotted in fig. S1 reveals distinct structures, the exact same features are present in the random selection of two products from the 3-body signal. The structure likely arises due to the intrinsic dynamics in the three-body reaction, which has one fragment taking a constant fraction of the energy in different channels. The residual signal does not support the presence of any peaks outside these features. Therefore, it is concluded that the reaction predominantly forms three products.

1.2 Three-body analysis

For three products, energy and momentum conservation allows a wide range of energy sharing, and the work of U. Müller, P. C. Cosby and co-workers, who derived a general model to describe the three-body fragmentation of H_3, is used as a basis for evaluation of these data [38]. The fraction of the available energy, E, that each particle carry can be described by two parameters a and b according to:

$$E_1 = aE, \qquad E_2 = bE, \qquad E_3 = cE \tag{S1}$$

where E_i are the kinetic energies of each one of the three products, and c=1-a-b. The momentum vectors can always be described to lie in an arbitrary plane, and can be defined as:

$$\vec{p}_1 = (p_{1x}, 0, 0)\,, \quad \vec{p}_2 = (p_{2x}, p_y, 0)\,, \vec{p}_3 = (-(p_{1x} + p_{2x}), -p_y, 0) \tag{S2}$$

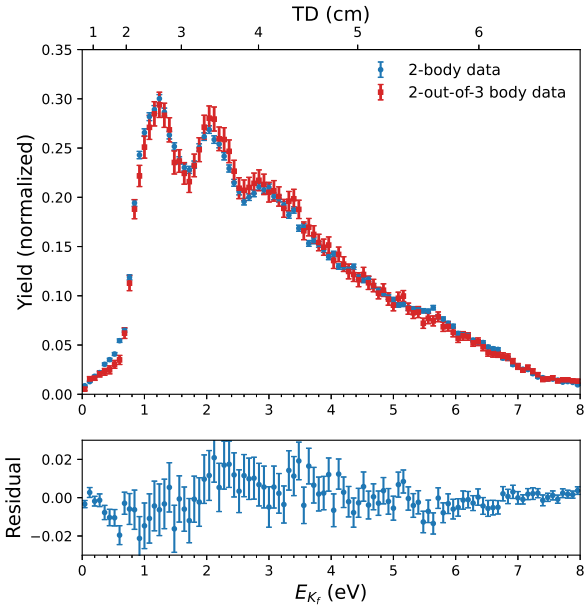

Fig. S1 E_{K_f} distributions for two-body coincidence data. The data indicated by the filled blue circles shows the measured two-body data, and the red filled circles the contribution from three-body data where one neutral product is randomly removed.

where p_{1x}, p_{2x} and p_y are defined as

$$p_{1x} = \sqrt{2aEm}, \quad p_{2x} = \frac{(1-2b-2a)Em}{p_{1x}}, \quad p_y = \sqrt{2mbE - p_{2x}^2} \tag{S3}$$

From energy and momentum conservation, the limits of a and b can be determined. Since the reaction can take place in a plane with any orientation in space, the vectors in the plane are then rotated randomly along both axes using rotation matrices. The displacement of each fragment from the center of mass due to the kinetic energy released, E, can then be derived:

$$\vec{r}_i = \frac{L}{v}\frac{\vec{p}_i}{m} \tag{S4}$$

where L is the distance to the interaction region, and v is the average velocity of the two ion beams. The total displacement (TD) of the fragments on the detector is then determined by:

$$TD = \sqrt{\sum_{i=1}^{3} \vec{r}_i^{\,2}} \tag{S5}$$

From this, the kinetic energy released in the reaction can be reconstructed:

$$E = \frac{1}{2}\, m \left(\frac{v \cdot TD}{L} \right)^2 \tag{S6}$$

This equation is exact, and would give results with smaller error bars, if the distance from the point of interaction, L, to the detector would be known with high precision. However, the reaction can happen at any point in the biased interaction region and the average distance is used to compute E, both in the experiment and in the simulation, which limits the energy resolution. The additional broadening due to the internal energy in the parent ions is simply implemented in the simulation by adding a Boltzmann distribution of energy to the initial kinetic energy release.

1.3 Three-body reaction dynamics

The dynamics of the reaction can then be evaluated based on the energy partitioning among the fragments, i.e parameters a and b in equation S1. For example, in the case of a linear break-up, $a = 0$, and the energy is shared equally between the two other fragments. This would be visible in a Dalitz plot, which represents the three energy fractions in a single two-dimensional plot. These are defined by the generalized coordinates [38]:

$$\eta_1 = \frac{E_1 - E_2}{\sqrt{3}E} \tag{S7a}$$

$$\eta_2 = \frac{2E_3 - E_2 - E_1}{3E} \tag{S7b}$$

Which due to energy and momentum conservation, confines all allowed geometries into a circle of a radius 1/3.

1.4 The free-rotor model in two-step reactions

In the case of a dissociation via an intermediate state, the reaction can be described as follows:

$$O_2^+ + O^- \rightarrow O_2^* + O + E_{K_i} \rightarrow O + O + O + E_{K_f}, \tag{S8}$$

i.e, there is an intermediate kinetic energy release E_{K_i} which leaves O_2 in an excited state, and there is a subsequent, final kinetic energy release, E_{K_f}, for the complete process which includes the kinetic energy released in the dissociation of O_2^*. Within the free-rotor model [8,45], we assume that the neutralised anion no longer participates in the reaction after the initial electron-transfer step, i.e. no further energy is then exchanged between O and O_2^*. The fraction of the available energy taken by the neutralised anion is then determined by the kinetic energy, E_{K_i}, released as the intermediate state O_2^* is formed. This fraction defines the value of parameter a in equation (S1) for a two-step process of the kind discussed here. As seen from the

center-of-mass of O_2^*, the kinetic energies of both O-atoms must be the same, and their momenta opposite. However, in the center-of-mass of all three atoms, the length of the momentum vectors may differ, and thus we measure different kinetic energies in the lab frame and in the center-of-mass of the complete system. To reflect this, the remaining energy is randomly distributed between the two other fragments, b and c. This effectively results in a line in the Dalitz plot, as can be inferred from the Dalitz coordinates.

From conservation of energy and momentum, the kinetic energy released when the intermediate state is formed is thus determined by the kinetic energy, E_O, of the neutralised anion:

$$E_{K_i} = \frac{3m_O}{2m_O} E_O \tag{S9}$$

This result is exact provided that the neutralised atomic anion can be correctly identified among the three separating O-atoms. Here, the three particles have the same mass, and specific selections are applied to aid the particular identification, based on the observed features in the Dalitz plots (see fig. 2 in the main text). For channel (1b), the kinetic energy release in the first step is much smaller than the kinetic energy release in the second step, and the neutralised oxygen anion most often takes on the smallest amount of energy. The opposite is true for channel (1d), and, in this case, the oxygen with the largest energy instead is selected. For channel (1c), no appropriate selection could be made. The miss-identification results in an apparent background associated with the E_{K_i} spectra. The same selection is implemented in the simulation to reproduce this background, and make an appropriate fit.

1.5 Vibrational cooling

As discussed in the main text, the vibrational lifetimes for the mixed $^{16,18}O_2^+$ isotopologue have been calculated to be on the order of seconds [37]. Using the data from ref. [37], the vibrational population as a function of storage time is shown in Fig. S2(a), and, after 60 s, a 95% ground-state population is expected. After about 30 s of storage, complete depletion of the higher vibrational states ($v \geq 4$) is expected, and, for both experimental and technical reasons, signals are analysed for the first 0-5 s and the last 30-60 s of storage. These are the data plotted in Fig. S2(b).

To obtain the branching fractions into the various channels for the later storage time data, a similar fitting procedure is undertaken as for the early data described in the main text. Figure S2(b) shows the fit of simulated distributions for the $^{16,18}O_2^+$ data set after 30 s of cooling. Here, the internal energy of the O_2^+ ions is described by a 1000 K vibrational Boltzmann distribution (while keeping the initial, unchanged 3000 K rotational population). As before, this describes the prominent experimental features well. What remains of the smaller channel is again only described by non-Boltzmann, individually-fit contributions.

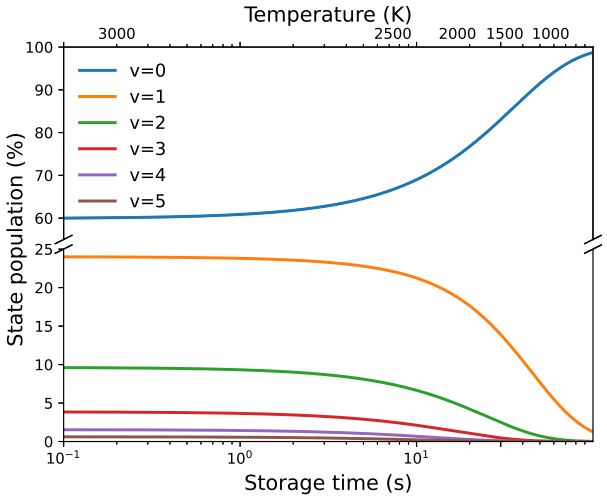

(a)

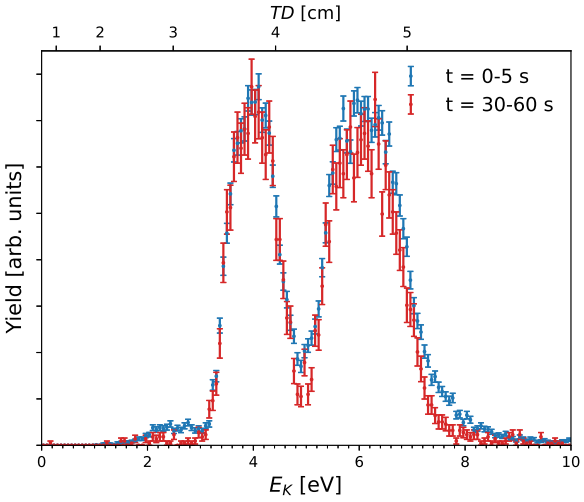

(b)

Fig. S2 (a) Calculated vibrational state distributions in $^{16,18}O_2^+$ as function of ion storage time with a starting temperature of 3000 K. DESIREE's ≈ 20 K radiation field [47] is neglected; (b) Coincident three-body total kinetic energy release, E_{K_f}, and Total Displacement, TD, distributions from MN of $^{16,18}O_2^+ + O^-$ for two different slices of ion-storage times.